Karlsruhe Institute of Technology

wave phenomena
analysis and numerics

Preconditioned implicit time integration schemes for Maxwell's equations on locally refined grids

Marlis Hochbruck, Jonas Köhler, Pratik M. Kumbhar

CRC Preprint 2022/29, June 2022

KARLSRUHE INSTITUTE OF TECHNOLOGY

CRC 1173

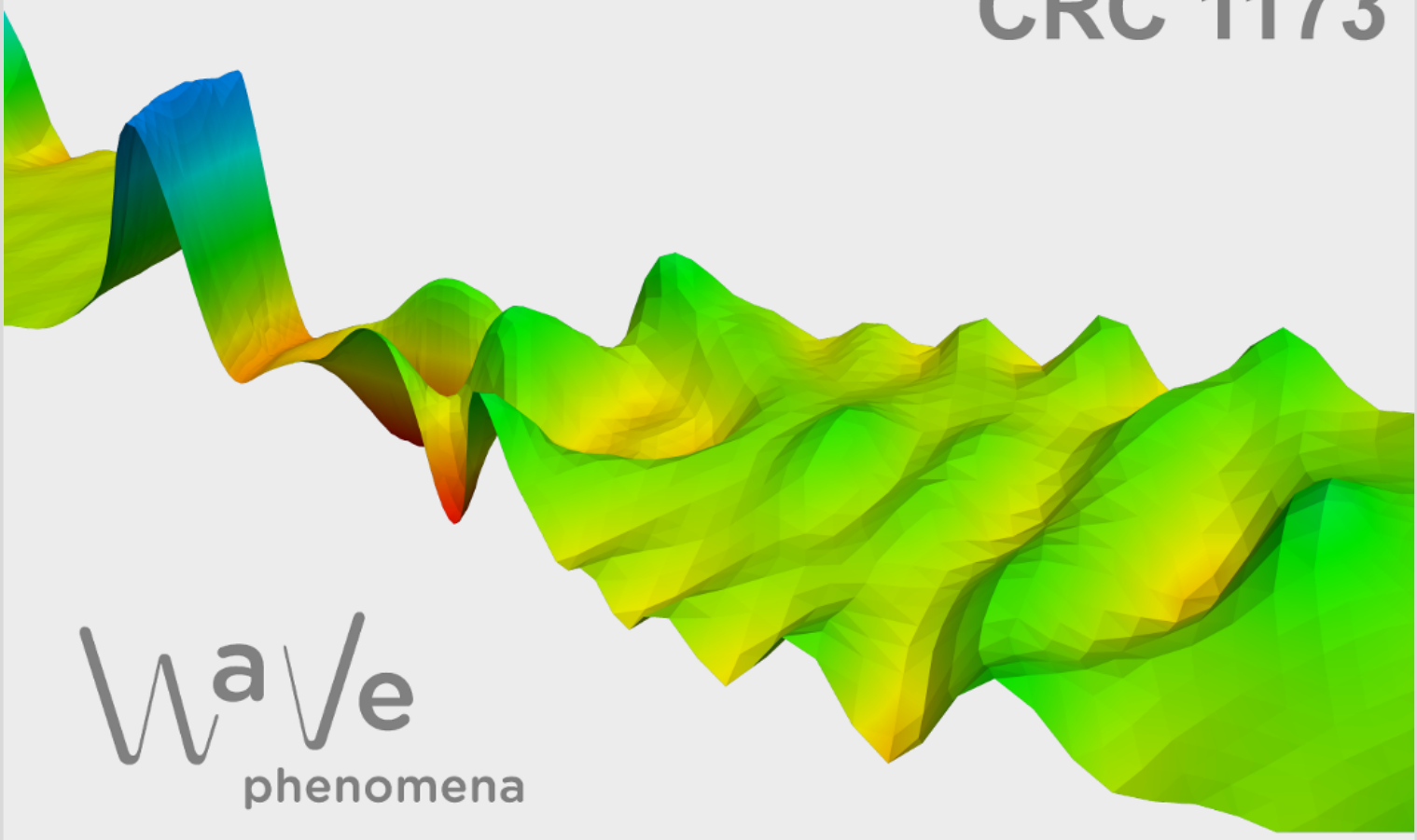

Participating universities

Universität Stuttgart

EBERHARD KARLS
UNIVERSITÄT
TÜBINGEN

Funded by

ISSN 2365-662X

PRECONDITIONED IMPLICIT TIME INTEGRATION SCHEMES FOR MAXWELL'S EQUATIONS ON LOCALLY REFINED GRIDS *

MARLIS HOCHBRUCK†, JONAS KÖHLER‡, AND PRATIK M. KUMBHAR§

Abstract. In this paper, we consider an efficient implementation of higher-order implicit time integration schemes for spatially discretized linear Maxwell's equations on locally refined meshes. In particular, our interest is in problems where only a few of the mesh elements are small while the majority of the elements is much larger. We suggest to approximate the solution of the linear systems arising in each time step by a preconditioned Krylov subspace method, e.g., the quasi-minimal residual method by Freund and Nachtigal [13].

Motivated by the analysis of locally implicit methods by Hochbruck and Sturm [25], we show how to construct a preconditioner in such a way that the number of iterations required by the Krylov subspace method to achieve a certain accuracy is bounded independently of the diameter of the small mesh elements. We prove this behavior by using Faber polynomials and complex approximation theory.

The cost to apply the preconditioner consists of the solution of a small linear system, whose dimension corresponds to the degrees of freedom within the fine part of the mesh (and its next coarse neighbors). If this dimension is small compared to the size of the full mesh, the preconditioner is very efficient.

We conclude by verifying our theoretical results with numerical experiments for the fourth-order Gauß-Legendre Runge–Kutta method.

Key words. Maxwell's equations, higher-order time integration, locally refined mesh, Krylov subspace methods, preconditioning, error analysis.

AMS subject classifications. 65F10, 65F08, 65L04, 65L06, 65M22

1. Introduction.

Maxwell's equations play a crucial role in understanding and analyzing electromagnetic waves. Though finite difference time-domain methods [32] are still predominately utilized to solve Maxwell's equations, numerous other methods based on finite element or finite volume space discretizations have been introduced and are gaining more and more importance.

The numerical solution of time dependent partial differential equations by a method of lines approach involves first discretization in space and then integrating the semi-discrete system in time. For the space discretization, discontinuous Galerkin (dG) methods (see [5] and references therein) are popular due to their flexibility in treating complex geometries and discontinuous material parameters. Since dG methods lead to block diagonal mass matrices, applying an explicit time integration scheme can be implemented very efficiently. Unfortunately, explicit time integration methods are subject to the so-called Courant-Friedrichs-Lewy (CFL) condition depending on the minimum diameter of mesh elements, denoted by $h_{\min}$, that is, the time step τ needs to satisfy $\tau \lesssim h_{\min}$. Here, we are interested in locally refined meshes, where most of the mesh elements are coarse but a very small number of mesh elements are fine. The latter require very small time steps on all mesh elements, which makes the computation inefficient. An alternative is to use implicit time integrators. These can eliminate the CFL condition completely but involve solving a linear system involving all degrees of freedom at each time step. Unfortunately, this is expensive and might

*version June 27, 2022.

Funding: Funded by the Deutsche Forschungsgemeinschaft (DFG, German Research Foundation) — Project-ID 258734477 — SFB 1173

†Karlsruhe Institute of Technology, Germany, (marlis.hochbruck@kit.edu).

‡Karlsruhe Institute of Technology, Germany, (jonas.koehler@kit.edu).

§Karlsruhe Institute of Technology, Germany, (pratik.kumbhar@kit.edu).

even not be feasible for large 3D problems.

To tackle this problem, locally implicit (LI) methods [31, 3, 25, 1, 4, 26] and local time stepping methods [28, 6, 16, 15] were introduced and studied. While there is a rigorous analysis of LI methods of order two for linear problems, it is not clear how to prove the stability for higher-order LI methods constructed via composition methods [18, Section II.4].

In this paper, we introduce a new strategy to develop a higher-order time integration method to solve linear Maxwell's equations on a locally refined spatial grid in a computationally efficient way. Note that though we only consider linear Maxwell's equations, our analysis can be applied to general Friedrich's system as well [20, 21].

We start with a higher-order implicit Runge-Kutta method. Due to the large size of the coefficient matrices, iterative solvers are usually used to solve the linear systems. These solvers in many cases require less memory, less total time, and have more scalable parallel performance. There have been numerous iterative methods which were discovered in the last few decades to solve a linear system. Here, we restrict ourselves to Krylov subspace methods (see [29] and references therein). We observe that the coefficient matrix resulting from the full discretization of the linear Maxwell's equations is complex symmetric, and hence we use the quasi-minimal residual (QMR) method to solve it [10, 13, 14]. Our main contribution is to construct a suitable preconditioner for the QMR method and to prove, that the number of iterations required to reach a certain accuracy is independent of the fine mesh.

The paper is organized as follows. In Section 2, we present our model problem, notations, and recall properties of curl matrices obtained through spatial discretization of Maxwell's equations. Section 3 is dedicated to higher-order implicit Runge-Kutta methods. In Section 4, we recall known results on Krylov subspace methods and prove how their efficiency can be improved by the proposed preconditioning. Finally in Section 5, we verify our theoretical findings with numerical experiments.

2. Problem setting. Let $\Omega \subset \mathbb{R}^d, d = 1, 2, 3$, be an open, bounded Lipschitz domain. For $T > 0$, let $H, E : (0, T) \times \Omega \to \mathbb{R}^d$ be the unknown magnetic and electric field respectively, and $J : (0, T) \times \Omega \to \mathbb{R}^d$ be the given electric field density. The linear Maxwell's equations in an isotropic medium with permeability $\mu : \Omega \to \mathbb{R}$, permittivity $\epsilon : \Omega \to \mathbb{R}$, and a perfect conducting boundary are given by

$$\mu \partial_t H = -\operatorname{curl} E, \qquad (0,T)\times\Omega, \tag{2.1a}$$

$$\epsilon \partial_t E = \operatorname{curl} H - J, \qquad (0,T)\times\Omega, \tag{2.1b}$$

$$H(0) = H^0, \quad E(0) = E^0, \qquad \Omega, \tag{2.1c}$$

$$n \times E = 0, \qquad (0,T)\times\partial\Omega, \tag{2.1d}$$

where ∂_t denotes the partial derivative with respect to time and n is the unit outward normal vector of the domain Ω. The initial conditions H^0 and E^0 satisfy

$$\operatorname{div}(\mu H^0) = 0, \quad \operatorname{div}(\mu E^0) = \varrho(0), \qquad \Omega, \tag{2.1e}$$

$$n \cdot (\mu H^0) = 0, \qquad \partial\Omega, \tag{2.1f}$$

where $\varrho(0)$ is the charge density at the initial time $t = 0$.

For a full discretization of (2.1), we first discretize it in space using a dG method with central fluxes on a suitable mesh $\mathcal{T}_h$ [5],[25, Section 2]. On this mesh we define the broken polynomial space $V_h = (\mathbb{P}_m(\mathcal{T}_h))^3$ consisting of piecewise polynomials of

degree at most m on each mesh element. The dG method then yields

$$\begin{aligned} \partial_t H_h &= -C_E\, E_h, && (0,T),\\ \partial_t E_h &= \quad C_H\, H_h - J_h, && (0,T),\\ H_h(0) &= H_h^0, \quad E_h(0) = E_h^0, \end{aligned} \tag{2.2}$$

where C_E and C_H are spatially discretized curl-operators containing μ and ε respectively, and H_h^0, E_h^0, and J_h are L^2 projections of H^0, E^0 and J respectively, onto V_h with respect to the weighted inner products defined below. The boundary condition (2.1d) is weakly enforced in the definition of C_E. These discrete operators C_E, C_H are constructed by using weighted L^2 inner products defined via

$$\big(u,v\big)_\mu = \big(\mu u, v\big)_{L^2(\Omega)}, \qquad \big(u,v\big)_\varepsilon = \big(\varepsilon u, v\big)_{L^2(\Omega)}, \qquad u,v \in L^2(\Omega).$$

The corresponding norms are denoted by $\big\|\cdot\big\|_\mu$ and $\big\|\cdot\big\|_\varepsilon$ respectively. We refer to [5, 25] for details on the dG discretization.

Let $\{\phi_1,\dots,\phi_N\}$ be a basis of V_h. Then the unknown discrete solutions $H_h, E_h : (0,T) \to V_h$ and the source term $J_h : (0,T) \to V_h$ can be represented as

$$H_h(t) = \sum_{j=1}^N H_j(t)\phi_j, \qquad E_h(t) = \sum_{j=1}^N E_j(t)\phi_j, \qquad J_h(t) = \sum_{j=1}^N J_j(t)\phi_j,$$

with coefficient vectors $\mathbf{H}(t) = (H_j(t))_{j=1}^N$, $\mathbf{E}(t) = (E_j(t))_{j=1}^N$, $\mathbf{J}(t) = (J_j(t))_{j=1}^N$. This results in mass and stiffness matrices given by

$$(\mathbf{M}_H)_{l,j} = \big(\phi_j,\phi_l\big)_\mu, \qquad (\widetilde{\mathbf{C}}_H)_{l,j} = \big(C_H\phi_j,\phi_l\big)_\varepsilon, \tag{2.3a}$$

$$(\mathbf{M}_E)_{l,j} = \big(\phi_j,\phi_l\big)_\varepsilon, \qquad (\widetilde{\mathbf{C}}_E)_{l,j} = \big(C_E\phi_j,\phi_l\big)_\mu. \tag{2.3b}$$

Then, for $t \in [0,T]$, (2.2) is equivalent to the following system of ordinary differential equations,

$$\begin{aligned} \partial_t \mathbf{H} &= -\mathbf{C}_E\, \mathbf{E}, && \mathbf{C}_E = \mathbf{M}_H^{-1}\widetilde{\mathbf{C}}_E,\\ \partial_t \mathbf{E} &= \quad \mathbf{C}_H\, \mathbf{H} - \mathbf{J}, && \mathbf{C}_H = \mathbf{M}_E^{-1}\widetilde{\mathbf{C}}_H,\\ \mathbf{H}(0) &= \mathbf{H}^0, \quad \mathbf{E}(0) = \mathbf{E}^0. \end{aligned} \tag{2.4}$$

Here, $\mathbf{H}^0$ and $\mathbf{E}^0$ are the coefficient vectors of H_h^0 and E_h^0 respectively.

With an abuse of notation, given $x_h, y_h \in V_h$ with coefficient vectors $\mathbf{x}, \mathbf{y} \in \mathbb{C}^N$, we define

$$\big(\mathbf{x},\mathbf{y}\big)_\varepsilon := \mathbf{y}^*\mathbf{M}_E\mathbf{x} = \big(x_h,y_h\big)_\varepsilon, \qquad \big(\mathbf{x},\mathbf{y}\big)_\mu := \mathbf{y}^*\mathbf{M}_H\mathbf{x} = \big(x_h,y_h\big)_\mu, \tag{2.5}$$

and do so analogously for the induced norms in $\mathbb{C}^N$. Here, $*$ denotes the conjugate transpose. For the matrix norms, we also take these weights into account, since then these norms are equivalent to the operator norms of the discrete operators C_H and C_E, i.e., we have

$$\big\|\mathbf{C}_H\big\|_{\varepsilon\leftarrow\mu} = \sup_{\mathbf{x}\in\mathbb{C}^N\setminus\{\mathbf{0}\}} \frac{\big\|\mathbf{C}_H\mathbf{x}\big\|_\varepsilon}{\big\|\mathbf{x}\big\|_\mu} = \sup_{x_h\in V_h\setminus\{0\}} \frac{\big\|C_H x_h\big\|_\varepsilon}{\big\|x_h\big\|_\mu} = \big\|C_H\big\|_{\varepsilon\leftarrow\mu}, \tag{2.6a}$$

$$\big\|\mathbf{C}_E\big\|_{\mu\leftarrow\varepsilon} = \sup_{\mathbf{x}\in\mathbb{C}^N\setminus\{\mathbf{0}\}} \frac{\big\|\mathbf{C}_E\mathbf{x}\big\|_\mu}{\big\|\mathbf{x}\big\|_\varepsilon} = \sup_{x_h\in V_h\setminus\{0\}} \frac{\big\|C_E x_h\big\|_\mu}{\big\|x_h\big\|_\varepsilon} = \big\|C_E\big\|_{\mu\leftarrow\varepsilon}. \tag{2.6b}$$

In this paper, we are interested in locally refined meshes. We refer to our earlier papers [25, 26] for detailed explanations on these meshes, but for the completion of this paper, we introduce the necessary notation here. A locally refined mesh is a mesh in which most of the mesh elements are coarse and very few mesh elements are fine. Let $\mathcal{T}_{h,c}$ and $\mathcal{T}_{h,f}$ denote the collection of all coarse and fine mesh elements, respectively. We denote by h_f and h_c the size of smallest mesh elements in $\mathcal{T}_{h,f}$ and in $\mathcal{T}_{h,c}$, respectively. These two sets are related to each other via

$$h_f \ll h_c \quad \text{and} \quad \operatorname{card}(\mathcal{T}_{h,f}) \ll \operatorname{card}(\mathcal{T}_{h,c}).$$

Based on this decomposition of the mesh, the matrices defined in (2.4) can be split into

$$\mathbf{C}_H = \mathbf{C}_H^i + \mathbf{C}_H^e, \qquad \mathbf{C}_E = \mathbf{C}_E^i + \mathbf{C}_E^e, \tag{2.7}$$

cf. [25] for more details. The indices i and e indicate that the elements on which $\mathbf{C}_H^i, \mathbf{C}_E^i$ act are treated implicitly and the ones on which $\mathbf{C}_H^e, \mathbf{C}_E^e$ act are integrated explicitly. In fact, it was shown in [25] that not only the fine elements have to be treated implicitly but also their direct coarse neighbors.

Let us state some properties of these matrices which are inherited from their corresponding discrete operators, cf. [25]. First, $\mathbf{C}_E$ and $\mathbf{C}_H$ are adjoint to each other, that is, for all $\mathbf{H}, \mathbf{E} \in \mathbb{C}^N$,

$$\big(\mathbf{C}_H\mathbf{H}, \mathbf{E}\big)_\varepsilon = \big(\mathbf{H}, \mathbf{C}_E\mathbf{E}\big)_\mu. \tag{2.8}$$

It is easy to verify that these split matrices preserve the adjointness property of their respective full ones, that is,

$$\big(\mathbf{C}_H^e\mathbf{H}, \mathbf{E}\big)_\varepsilon = \big(\mathbf{H}, \mathbf{C}_E^e\mathbf{E}\big)_\mu, \qquad \big(\mathbf{C}_H^i\mathbf{H}, \mathbf{E}\big)_\varepsilon = \big(\mathbf{H}, \mathbf{C}_E^i\mathbf{E}\big)_\mu. \tag{2.9}$$

In addition to this, they satisfy

$$\mathbf{C}_H^e\mathbf{C}_E^e = \mathbf{C}_H^e\mathbf{C}_E, \qquad \mathbf{C}_H^i\mathbf{C}_E^i = \mathbf{C}_H^i\mathbf{C}_E. \tag{2.10}$$

Furthermore, combining the above properties, it holds

$$\big\|\mathbf{C}_E\mathbf{E}\big\|_\mu^2 = \big\|\mathbf{C}_E^e\mathbf{E}\big\|_\mu^2 + \big\|\mathbf{C}_E^i\mathbf{E}\big\|_\mu^2. \tag{2.11}$$

One of the important results from [25] is that the explicit split matrices $\mathbf{C}_H^e$ and $\mathbf{C}_E^e$ can be bounded independently of the fine mesh, that is, using the definition of weighted norm in (2.6) we have

$$\big\|\mathbf{C}_E^e\big\|_{\mu\leftarrow\varepsilon} \le ch_c^{-1}, \qquad \big\|\mathbf{C}_H^e\big\|_{\varepsilon\leftarrow\mu} \le ch_c^{-1}, \tag{2.12}$$

with a constant c that is independent of h_f and h_c.

In [25, 26], these split matrices were constructed to develop a locally implicit time integration method. In this paper, we use these split matrices in a different way: to construct preconditioners which improve the performance of Krylov subspace methods.

3. Higher-order implicit Runge–Kutta methods. In this section, we consider the time integration of (2.4) by an s-stage implicit Runge–Kutta (RK) methods given by its matrix $\boldsymbol{\mathcal{O}} = (a_{ij})_{i,j=1}^{s}$, weights b_i and nodes c_i, $i = 1, \dots, s$, cf., [18, Section II.1]. To simplify the presentation, we write (2.4) in the compact form

$$\begin{aligned} \partial_t \mathbf{u} &= \mathbf{C}\mathbf{u} + \mathbf{j}, \qquad (0,T), \\ \mathbf{u}^0 &= \mathbf{u}(0), \end{aligned} \tag{3.1}$$

where

$$\mathbf{u} = \begin{pmatrix} \mathbf{H} \\ \mathbf{E} \end{pmatrix}, \quad \mathbf{j} = \begin{pmatrix} \mathbf{0} \\ -\mathbf{J} \end{pmatrix} \in \mathbb{R}^{2N}, \quad \text{and} \quad \mathbf{C} = \begin{pmatrix} \mathbf{0} & -\mathbf{C}_E \\ \mathbf{C}_H & \mathbf{0} \end{pmatrix} \in \mathbb{R}^{(2N)\times(2N)}.$$

Assume that we already computed an approximation $\mathbf{u}^n \approx \mathbf{u}(t_n)$ at time $t_n = n\tau$, where $\tau > 0$ denotes the step size. Then, the implicit Runge–Kutta method applied to (3.1) leads to the following coupled linear system of equations for the intermediate stages $\mathbf{U}_i \approx \mathbf{u}(t_n + c_i\tau)$

$$\mathbf{U}_i = \mathbf{u}^n + \tau \sum_{j=1}^{s} a_{ij}\big(\mathbf{C}\mathbf{U}_j + \mathbf{F}_j\big), \quad i = 1, \dots, s, \tag{3.2}$$

where $\mathbf{F}_j = \mathbf{j}(t_n + c_j\tau)$. The new approximation $\mathbf{u}^{n+1} \approx \mathbf{u}(t_{n+1})$ is then given explicitly by

$$\mathbf{u}^{n+1} = \mathbf{u}^n + \tau \sum_{i=1}^{s} b_i\big(\mathbf{C}\mathbf{U}_i + \mathbf{F}_i\big). \tag{3.3}$$

3.1. Gauß collocation methods. We use Gauß collocation methods to construct higher-order implicit RK methods. It is well known that these methods are algebraically stable [19, Theorem IV.12.9] and the RK matrix $\boldsymbol{\mathcal{O}}$ is invertible [19, Section IV.14]. In addition, the error analysis for linear wave-type problems [24, Section 3.1] makes use of the existence of a diagonal positive definite matrix $\widehat{\mathbf{D}}$ and a positive scalar $\eta > 0$ such that

$$\mathbf{v}^\top \widehat{\mathbf{D}} \boldsymbol{\mathcal{O}}^{-1} \mathbf{v} \geq \eta \mathbf{v}^\top \widehat{\mathbf{D}} \mathbf{v}, \quad \text{for all} \quad \mathbf{v} \in \mathbb{R}^s. \tag{3.4}$$

Here, $^\top$ denotes the transpose. For Gauß collocation methods, the coercitivity condition (3.4) is satisfied for $\widehat{\mathbf{D}} = \widehat{\mathbf{B}}(\widehat{\mathbf{C}}^{-1} - \mathbf{I}_s)$, where $\widehat{\mathbf{B}} := \operatorname{diag}(b_1, \dots, b_s)$, $\widehat{\mathbf{C}} := \operatorname{diag}(c_1, \dots, c_s)$, and $\mathbf{I}_s$ is the identity matrix of size s, cf. [19, Theorem IV.14.5].

For an efficient implementation of (3.2), we use Kronecker products [18, Section VIII.6] to rewrite it as

$$\mathbf{U} = \mathbb{1}_s \otimes \mathbf{u}^n + \tau\big((\boldsymbol{\mathcal{O}} \otimes \mathbf{C})\mathbf{U} + (\boldsymbol{\mathcal{O}} \otimes \mathbf{I}_{2N})\mathbf{F}\big), \tag{3.5}$$

where $\mathbf{U} = (\mathbf{U}_i)_{i=1}^{s}$, $\mathbf{F} = \big(\mathbf{F}_i\big)_{i=1}^{s} \in \mathbb{C}^{2Ns}$, $\mathbf{I}_{2N}$ is the identity matrix of size $2N$, and the term $\mathbb{1}_s$ denotes the vector in $\mathbb{R}^s$ consisting of all ones. Diagonalization of $\boldsymbol{\mathcal{O}}$ yields a nonsingular matrix $\mathbf{T} \in \mathbb{C}^{s\times s}$ containing the eigenvectors and a diagonal matrix $\boldsymbol{\Lambda}_{\mathcal{O}} \in \mathbb{C}^{s\times s}$ containing eigenvalues λ_i, such that

$$\mathbf{T}^{-1}\boldsymbol{\mathcal{O}}\mathbf{T} = \boldsymbol{\Lambda}_{\mathcal{O}}, \qquad \boldsymbol{\Lambda}_{\mathcal{O}} = \operatorname{diag}(\lambda_1, \dots, \lambda_s). \tag{3.6}$$

Substituting $\boldsymbol{\mathcal{O}} = \mathbf{T}\boldsymbol{\Lambda}_{\mathcal{O}}\mathbf{T}^{-1}$ in (3.5) and performing some Kronecker product operations leads to s decoupled linear systems of the form

$$(\mathbf{I}_s \otimes \mathbf{I}_{2N} - \tau(\boldsymbol{\Lambda}_{\mathcal{O}} \otimes \mathbf{C}))\mathbf{Z} = \mathbf{Z}^0 + \tau(\boldsymbol{\Lambda}_{\mathcal{O}} \otimes \mathbf{I}_{2N})\widetilde{\mathbf{F}}, \tag{3.7}$$

where,

$$\mathbf{Z} = (\mathbf{T}^{-1} \otimes \mathbf{I}_{2N})\mathbf{U}, \quad \mathbf{Z}^0 = (\mathbf{T}^{-1} \otimes \mathbf{I}_{2N})(\mathbb{1}_s \otimes \mathbf{u}^n), \quad \widetilde{\mathbf{F}} = (\mathbf{T}^{-1} \otimes \mathbf{I}_{2N})\mathbf{F}. \tag{3.8}$$

Note that $\boldsymbol{\mathcal{O}}$ might have complex conjugate pairs of eigenvalues. For such eigenvalues (say $\lambda_j = \overline{\lambda_i}$), the corresponding linear systems are

$$(\mathbf{I}_{2N} - \tau\lambda_i\mathbf{C})\mathbf{Z}_i = \mathbf{Z}_i^0 + \tau\lambda_i\widetilde{\mathbf{F}}_i, \tag{3.9a}$$

$$(\mathbf{I}_{2N} - \tau\overline{\lambda_i}\,\mathbf{C})\mathbf{Z}_j = \mathbf{Z}_j^0 + \tau\overline{\lambda_i}\,\widetilde{\mathbf{F}}_j. \tag{3.9b}$$

In the homogeneous case, i.e., $\mathbf{J} \equiv 0$ which leads to $\widetilde{\mathbf{F}} \equiv 0$, the first term on the right-hand sides of (3.9a) and (3.9b) are conjugate to each other and so are the solutions.

LEMMA 3.1. *If $\mathbf{J} \equiv 0$ and $\lambda_j = \overline{\lambda_i}$, then the solutions of (3.9) satisfy $\mathbf{Z}_j = \overline{\mathbf{Z}}_i$.*

Proof. The RK matrix $\boldsymbol{\mathcal{O}}$ is real and thus complex eigenvalues and eigenvectors appear in complex conjugate pairs. Hence there exists a symmetric permutation matrix $\widehat{\mathbf{P}} \in \mathbb{R}^{s\times s}$ s.t.,

$$\overline{\mathbf{T}} = \mathbf{T}\widehat{\mathbf{P}}, \qquad \overline{\boldsymbol{\Lambda}_{\mathcal{O}}} = \widehat{\mathbf{P}}\boldsymbol{\Lambda}_{\mathcal{O}}\widehat{\mathbf{P}}, \tag{3.10}$$

which implies $\mathbf{T}^{-1} = \widehat{\mathbf{P}}\overline{\mathbf{T}^{-1}}$. We choose an arbitrary index $i \in \{0, \dots, s\}$ corresponding to a complex eigenvalue $\lambda_i \notin \mathbb{R}$ and define the index j such that $\mathbf{e}_j = \widehat{\mathbf{P}}\mathbf{e}_i$. By (3.8) and $\mathbf{u}^n \in \mathbb{R}^{2N}$ we have

$$\overline{\mathbf{Z}}_i^0 = (\mathbf{e}_i^\top \otimes \mathbf{I}_{2N})\overline{\mathbf{Z}}^0 = (\mathbf{e}_i^\top \overline{\mathbf{T}^{-1}}\mathbb{1}_s \otimes \mathbf{u}^n) = ((\widehat{\mathbf{P}}\mathbf{e}_i)^\top \mathbf{T}^{-1}\mathbb{1}_s) \otimes \mathbf{u}^n = \mathbf{Z}_j^0. \tag{3.11}$$

Conjugating (3.9a) proves that $\overline{\mathbf{Z}}_i$ solves (3.9b). ∎

In addition to this, $\mathbf{Z}_i$ and $\widetilde{\mathbf{F}}_i$ in (3.9a) can be further decomposed into

$$\mathbf{Z}_i = \begin{pmatrix} \mathbf{Z}_{H,i} \\ \mathbf{Z}_{E,i} \end{pmatrix}, \quad \widetilde{\mathbf{F}}_i = \begin{pmatrix} \mathbf{0} \\ \widetilde{\mathbf{F}}_{E,i} \end{pmatrix},$$

where $\mathbf{Z}_{H,i}, \mathbf{Z}_{E,i}$ denote unknowns corresponding to the transformed intermediate stages of $\mathbf{H}$ and $\mathbf{E}$ respectively. Taking the Schur complement, the linear systems in (3.9a) can be further reduced to

$$(\mathbf{I}_N + \alpha_i\,\mathbf{C}_H\mathbf{C}_E)\mathbf{Z}_{E,i} = \mathbf{Z}_{E,i}^0 + \tau\lambda_i(\mathbf{C}_H\mathbf{Z}_{H,i}^0 + \widetilde{\mathbf{F}}_{E,i}), \qquad \alpha_i := \tau^2\lambda_i^2 \in \mathbb{C}, \tag{3.12}$$

to compute the E-component of $\mathbf{Z}_i$. After solving this linear system of dimension N, the H-component of $\mathbf{Z}_i$ can be calculated explicitly via

$$\mathbf{Z}_{H,i} = \mathbf{Z}_{H,i}^0 - \tau\lambda_i\mathbf{C}_E\mathbf{Z}_{E,i}. \tag{3.13}$$

An efficient implementation of an s-stage implicit Runge-Kutta method using Gauß collocation points thus requires solving a linear system of the form

$$\mathbf{A}\mathbf{x} = \mathbf{b} \quad \text{where} \quad \mathbf{A} := \mathbf{I}_N + \alpha\,\mathbf{C}_H\mathbf{C}_E, \tag{3.14}$$

with a complex parameter $\alpha \in \mathbb{C}$, in each time step. The adjointness property (2.8) implies that $\mathbf{C}_H\mathbf{C}_E$ is symmetric with respect to $\big(\cdot,\cdot\big)_\varepsilon$ defined in (2.5). Hence, $\mathbf{A}$ is complex symmetric, that is,

$$\big(\mathbf{A}\mathbf{x},\mathbf{x}\big)_\varepsilon = \big(\mathbf{x},\overline{\mathbf{A}}\mathbf{x}\big)_\varepsilon, \qquad \mathbf{x}\in\mathbb{C}^N.$$

However, for $\alpha \notin \mathbb{R}$ it follows immediately that $\mathbf{A} \neq \mathbf{A}^*$ with respect to $\big(\cdot,\cdot\big)_\varepsilon$. If $\alpha \in \mathbb{R}$, then $\mathbf{A} \in \mathbb{R}^{N\times N}$ is symmetric. Moreover, for

$$\alpha \in \mathbb{C}\backslash\{z\in\mathbb{R} : z < 0\}, \tag{3.15}$$

the matrix $\mathbf{A}$ is invertible. For Gauß collocation methods, the coercivity condition (3.4) guarantees that the eigenvalues of $\boldsymbol{\mathcal{O}}$ are not purely imaginary, and hence (3.15) is satisfied.

4. Preconditioned Krylov subspace methods. In this section, we aim at designing a tailored preconditioner for solving the sparse linear system (3.14) by a preconditioned Krylov subspace method. We will prove that the number of Krylov iterations to achieve a certain tolerance is independent of the fine mesh. The overall method can be considered as a locally implicit scheme, because it only requires the solution of a small linear system as it is required for the second-order method in [25].

We remark that in Subsection 4.1, we consider the L^2 inner products and norms, but this analysis holds in any weighted inner products.

4.1. Krylov subspace methods for complex symmetric matrices. For a nonsingular, complex symmetric matrix $\mathbf{K} = \mathbf{K}^\top \in \mathbb{C}^{N\times N}$ and a given vector $\mathbf{f} \in \mathbb{C}^N$, we consider the linear system

$$\mathbf{K}\mathbf{x} = \mathbf{f}. \tag{4.1}$$

Given an initial guess $\mathbf{x}_0 \in \mathbb{C}^N$ and its initial residual vector $\mathbf{r}_0 = \mathbf{f} - \mathbf{K}\mathbf{x}_0$, a Krylov subspace method yields an approximation of the form

$$\mathbf{x}_m = \mathbf{x}_0 + \mathbf{W}_m\mathbf{y}_m, \qquad m = 1,2,\dots, \tag{4.2}$$

where $\mathbf{W}_m \in \mathbb{C}^{N\times m}$ is a basis of the mth Krylov subspace

$$\mathcal{K}_m(\mathbf{K},\mathbf{r}_0) := \operatorname{span}(\mathbf{r}_0,\mathbf{K}\mathbf{r}_0,\dots,\mathbf{K}^{m-1}\mathbf{r}_0),$$

and $\mathbf{y}_m \in \mathbb{C}^m$ is a suitable coefficient vector. The choices of $\mathbf{W}_m$ and $\mathbf{y}_m$ characterize the Krylov subspace method, cf. [11, 17, 29] for more details.

To exploit the complex symmetric structure of $\mathbf{K}$, we suggest to use the quasi-minimal residual (QMR) algorithm for complex symmetric matrices [10, Section 3], which is based on the complex symmetric Lanczos process. Here, $\mathbf{W}_m$ satisfies

$$\mathbf{K}\mathbf{W}_m = \mathbf{W}_{m+1}\widetilde{\mathbf{H}}_m, \qquad \mathbf{D}_{m+1}\widetilde{\mathbf{H}}_m = \mathbf{W}_{m+1}^\top\mathbf{K}\mathbf{W}_m, \tag{4.3}$$

with a diagonal matrix $\mathbf{D}_{m+1} = \mathbf{W}_{m+1}^\top\mathbf{W}_{m+1} \in \mathbb{C}^{(m+1)\times(m+1)}$. The complex symmetry of $\mathbf{K}$ implies that $\widetilde{\mathbf{H}}_m \in \mathbb{C}^{(m+1)\times m}$ is tridiagonal and the upper $m\times m$ submatrix of $\mathbf{D}_{m+1}\widetilde{\mathbf{H}}_m$ is again complex symmetric. $\widetilde{\mathbf{H}}_m$ has full column rank m until $\mathcal{K}_m(\mathbf{K},\mathbf{r}_0)$ becomes a $\mathbf{K}$-invariant subspace.

With $\beta = \|\mathbf{r}_0\|$, the QMR approximation is defined as

$$\mathbf{x}_m = \mathbf{x}_0 + \mathbf{W}_m\mathbf{y}_m, \qquad \mathbf{y}_m = \beta\widetilde{\mathbf{H}}_m^+\mathbf{e}_1, \qquad \widetilde{\mathbf{H}}_m^+ = (\widetilde{\mathbf{H}}_m^*\widetilde{\mathbf{H}}_m)^{-1}\widetilde{\mathbf{H}}_m^*, \tag{4.4}$$

where $\mathbf{e}_1$ denotes the first canonical unit vector. Its residual can be written as

$$\mathbf{r}_m = \mathbf{f} - \mathbf{K}\mathbf{x}_m = \mathbf{W}_{m+1}(\beta\mathbf{e}_1 - \widetilde{\mathbf{H}}_m\mathbf{y}_m).$$

The advantage of this algorithm compared to methods based on the Arnoldi process (e.g., GMRES) is that it uses three-term recurrences for the computation of the basis as well as for the approximation. It can be combined with look-ahead strategies [12] to prevent breakdowns of the Lanczos process, which might appear because it constructs a basis which is orthogonal w.r.t. the indefinite bilinear form $\langle \mathbf{x}, \mathbf{y}\rangle = \mathbf{x}^\top\mathbf{y}$, instead of the Euclidean inner product $\big(\mathbf{x}, \mathbf{y}\big) = \mathbf{x}^*\mathbf{y}$, see [10, Section 4]. For the sake of presentation, we assume that breakdowns do not appear until a sufficiently accurate solution is computed, but we note that with minor modifications, our analysis also holds for the (complex symmetric) look-ahead Lanczos method [12]. This assumption ensures that

$$\big\|\mathbf{D}_{m+1}^{-1}\big\| \le \delta, \tag{4.5}$$

for a given (small) tolerance $\delta > 0$, because otherwise, one would switch to the look-ahead version of the Lanczos process.

In the following, $\mathbb{P}_m$ denotes the set of all polynomials over $\mathbb{C}$ of degree at most m.

THEOREM 4.1. *Let $\mathbf{K}$ be a nonsingular, complex symmetric matrix, and $\mathbf{x}_m$ be the QMR approximation (4.4) after m steps. Then the error of the QMR method satisfies*

$$\big\|\mathbf{K}^{-1}\mathbf{f} - \mathbf{x}_m\big\| \le \big\|\mathbf{K}^{-1}\mathbf{P}_m\big\| \min_{\substack{p_m\in\mathbb{P}_m\\ p_m(0)=1}} \big\|p_m(\mathbf{K})\mathbf{r}_0\big\| \tag{4.6}$$

with a projection matrix $\mathbf{P}_m$ given by

$$\mathbf{P}_m = \mathbf{I}_N - \mathbf{W}_{m+1}\widetilde{\mathbf{H}}_m\widetilde{\mathbf{H}}_m^{+}\mathbf{D}_{m+1}^{-1}\mathbf{W}_{m+1}^\top.$$

Moreover, if $\big\|\mathbf{W}_{m+1}\mathbf{e}_j\big\| = 1$, $j = 1, \dots, m+1$, and (4.5) holds, we have

$$\big\|\mathbf{P}_m\big\| \le 1 + (m+1)\delta. \tag{4.7}$$

Proof. Analogously to the proof of [23, Theorem 2] it can be seen from (4.3) that $\mathbf{P}_m\mathbf{K}\mathbf{W}_m = 0$. Using (4.4) this implies

$$\mathbf{K}^{-1}\mathbf{f} - \mathbf{x}_m = \mathbf{K}^{-1}\mathbf{P}_m\mathbf{r}_0 = \mathbf{K}^{-1}\mathbf{P}_m p_m(\mathbf{K})\mathbf{r}_0$$

for all $p_m \in \mathbb{P}_m$ with $p_m(0) = 1$.

The bound on $\big\|\mathbf{P}_m\big\|$ follows from (4.5) and $\big\|\mathbf{W}_m\big\| \le \sqrt{m}$. ∎

Since $\big\|p_m(\mathbf{K})\mathbf{r}_0\big\| \le \big\|p_m(\mathbf{K})\big\|\big\|\mathbf{r}_0\big\|$, it remains to bound

$$\min_{\substack{p_m\in\mathbb{P}_m\\ p_m(0)=1}} \big\|p_m(\mathbf{K})\big\|.$$

This can be done by means of Faber polynomials and complex approximation theory, cf. [9], based on a superset of the field of values of $\mathbf{K}$ defined as

$$\mathcal{F}(\mathbf{K}) := \{\rho_{\mathbf{K}}(\mathbf{v}), \mathbf{v} \in \mathbb{C}^N, \mathbf{v} \neq \mathbf{0}\}, \qquad \rho_{\mathbf{K}}(\mathbf{v}) := \frac{\big(\mathbf{v}, \mathbf{K}\mathbf{v}\big)}{\big(\mathbf{v}, \mathbf{v}\big)}.$$

THEOREM 4.2. *Let $\mathcal{S} \subset \mathbb{C}$ be a convex and bounded superset of $\mathcal{F}(\mathbf{K})$ with $0 \notin \mathcal{S}$ and let ϕ be the conformal map which maps the exterior of $\mathcal{S}$ onto the exterior of the unit circle with $\phi(\infty) = \infty$. Then*

$$\min_{\substack{p_m \in \mathbb{P}_m \\ p_m(0)=1}} \big\|p_m(\mathbf{K})\big\| \le (1+\sqrt{2}) \min\Big\{ \frac{3}{\big|\phi(0)\big|^m}, \frac{2}{\big|\phi(0)\big|^m - 1} \Big\}. \tag{4.8}$$

Proof. It was shown in [2] that

$$\big\|p_m(\mathbf{K})\big\| \le (1+\sqrt{2}) \max_{z \in \mathcal{S}} \big|p_m(z)\big|.$$

The statement then follows from [22, Eq. (2.14)] and [9, Theorem 2]. ∎

The conformal map ϕ can be determined numerically by using the Schwarz-Christoffel toolbox [8].

4.2. Preconditioning for locally refined grids. Our aim and the content of this section is the construction of a preconditioner such that the field of values of the preconditioned matrix with respect to the weighted inner product $\big(\cdot,\cdot\big)_\varepsilon$ is independent of the fine mesh elements. Then by Theorem 4.2, the same holds for the error of the preconditioned Krylov method in this weighted inner product.

Motivated by locally implicit methods for Maxwell's equations in [25, 31], we suggest to precondition $\mathbf{A}$ from (3.14) with its dominant part,

$$\mathbf{A} \approx \mathbf{B} := \mathbf{I}_N + \gamma\, \mathbf{C}_H^i \mathbf{C}_E^i, \tag{4.9}$$

where $\gamma > 0$ is a suitably chosen parameter. Note that this basically boils down to replacing the curl matrices $\mathbf{C}_H, \mathbf{C}_E$ in (3.14) defined on the full mesh by the split matrices acting on the implicitly treated mesh elements, cf. Section 2. By (2.9) and $\gamma > 0$, the preconditioner $\mathbf{B}$ is symmetric and positive definite with respect to $\big(\cdot,\cdot\big)_\varepsilon$, and thus it has a symmetric and positive definite square root $\mathbf{B}^{1/2}$. This allows us to define an equivalent preconditioned linear system

$$\widetilde{\mathbf{A}}\widetilde{\mathbf{x}} = \widetilde{\mathbf{b}}, \tag{4.10a}$$

where

$$\widetilde{\mathbf{A}} := \mathbf{B}^{-1/2}\mathbf{A}\mathbf{B}^{-1/2}, \quad \widetilde{\mathbf{x}} := \mathbf{B}^{1/2}\mathbf{x} \quad \text{and} \quad \widetilde{\mathbf{b}} := \mathbf{B}^{-1/2}\mathbf{b}. \tag{4.10b}$$

Since $\mathbf{A}$ is complex symmetric and $\mathbf{B}$ is real symmetric, the preconditioned matrix $\widetilde{\mathbf{A}}$ is again complex symmetric (with respect to $\big(\cdot,\cdot\big)_\varepsilon$).

We now apply the complex symmetric QMR method to the preconditioned linear system (4.10) and refer to this method as the preconditioned QMR (pQMR) method, cf. [14, Alg. 8.1.]. It is essential that $\mathbf{B}^{1/2}$ is only used for theoretical purposes since its computation is usually too expensive. The implementation of this method only requires the solution of linear systems with $\mathbf{B}$ but does not involve the computation of $\mathbf{B}^{1/2}$ or $\mathbf{B}^{-1/2}$. Solving linear systems with $\mathbf{B}$ does not lead to too much overhead costs because $\mathbf{C}_H^i \mathbf{C}_E^i$ only acts on the fine elements and their direct neighbors and thus is of small dimension compared to $\mathbf{A}$.

It remains to show that its error can indeed be bounded independently of the fine mesh. Note that Theorems 4.1 and 4.2. also hold for $\|\cdot\| = \|\cdot\|_\varepsilon$, if the Lanczos process and the field of values are defined w.r.t. $\big(\cdot,\cdot\big) = \big(\cdot,\cdot\big)_\varepsilon$. Using these theorems,

it is sufficient to show that the field of values $\mathcal{F}(\widetilde{\mathbf{A}})$ can be bounded independent of the fine mesh.

Let

$$\alpha := \alpha_R + i\alpha_I, \quad \alpha_R, \alpha_I \in \mathbb{R}, \tag{4.11}$$

and

$$\Gamma^e_\zeta = 1 + \zeta \big\|\mathbf{C}^e_E\big\|^2_{\mu\leftarrow\varepsilon}, \qquad \Gamma^i_\zeta = 1 + \zeta \big\|\mathbf{C}^i_E\big\|^2_{\mu\leftarrow\varepsilon}, \quad \text{for } \zeta \in \mathbb{C}. \tag{4.12}$$

Defining quadrilaterals

$$Q = \operatorname{conv}\big\{1,\ \Gamma^e_\alpha, \frac{\alpha}{\gamma},\ \frac{\alpha}{\gamma}\Gamma^e_\gamma\big\}, \tag{4.13a}$$

$$R = \operatorname{conv}\big\{1,\ \Gamma^e_\gamma,\ 1 + \big(\frac{\alpha}{\gamma} - 1\big)\big(\Gamma^e_\gamma - \frac{1}{\Gamma^i_\gamma}\big),\ \Gamma^e_\gamma + \big(\frac{\alpha}{\gamma} - 1\big)\big(\Gamma^e_\gamma - \frac{1}{\Gamma^i_\gamma}\big)\big\}, \tag{4.13b}$$

allows us to construct a superset of $\mathcal{F}(\widetilde{\mathbf{A}})$ which is independent of the fine mesh.

THEOREM 4.3. *Let $\alpha \neq 0$ satisfy (3.15) and let $\widetilde{\mathbf{A}}$ be defined in (4.10b) where the preconditioner $\mathbf{B}$ is given in (4.9) for some parameter $\gamma > 0$. Then we have $\mathcal{F}(\widetilde{\mathbf{A}}) \subset S$, where*

$$S = \begin{cases} Q \cap R, & \alpha_I \neq 0, \\ [\frac{\alpha}{\gamma}, \Gamma^e_\alpha], & \alpha_I = 0, \quad 0 < \alpha_R = \alpha \leq \gamma, \\ [1, \frac{\alpha}{\gamma}\Gamma^e_\gamma], & \alpha_I = 0, \quad 0 < \gamma \leq \alpha_R = \alpha, \end{cases}$$

is independent of the fine mesh and $0 \notin S$.

Proof. Let $\mathbf{v} \in \mathbb{C}^N, \mathbf{v} \neq \mathbf{0}$ and $\widetilde{\mathbf{v}} := \mathbf{B}^{1/2}\mathbf{v}$. Then, by the symmetry of $\mathbf{B}$ (and thus of $\mathbf{B}^{1/2}$), the adjointness and split properties (2.8), (2.9), and (2.11), we have

$$\big(\widetilde{\mathbf{v}}, \widetilde{\mathbf{A}}\widetilde{\mathbf{v}}\big)_\varepsilon = \big(\mathbf{v}, \mathbf{A}\mathbf{v}\big)_\varepsilon = \big\|\mathbf{v}\big\|^2_\varepsilon + (\alpha_R + \mathrm{i}\,\alpha_I)\big(\big\|\mathbf{C}^e_E\mathbf{v}\big\|^2_\mu + \big\|\mathbf{C}^i_E\mathbf{v}\big\|^2_\mu\big), \tag{4.14a}$$

$$\big(\widetilde{\mathbf{v}}, \widetilde{\mathbf{v}}\big)_\varepsilon = \big(\mathbf{v}, \mathbf{B}\mathbf{v}\big)_\varepsilon = \big\|\mathbf{v}\big\|^2_\varepsilon + \gamma\big\|\mathbf{C}^i_E\mathbf{v}\big\|^2_\mu. \tag{4.14b}$$

We now distinguish the cases of α being real or complex.

(a) For $\alpha_I \neq 0$, it is easy to see that

$$1 \leq \operatorname{Re}\rho_{\widetilde{\mathbf{A}}}(\widetilde{\mathbf{v}}) + \frac{\gamma - \alpha_R}{\alpha_I}\operatorname{Im}\rho_{\widetilde{\mathbf{A}}}(\widetilde{\mathbf{v}}) = 1 + \frac{\gamma\big\|\mathbf{C}^e_E\mathbf{v}\big\|^2_\mu}{\big\|\mathbf{v}\big\|^2_\varepsilon + \gamma\big\|\mathbf{C}^i_E\mathbf{v}\big\|^2_\mu} \leq \Gamma^e_\gamma. \tag{4.15a}$$

The first inequality is obvious and the second follows from the definition of the weighted matrix norm in (2.6) and $\gamma > 0$. In addition, we have

$$0 \leq \operatorname{Re}\rho_{\widetilde{\mathbf{A}}}(\widetilde{\mathbf{v}}) - \frac{\alpha_R}{\alpha_I}\operatorname{Im}\rho_{\widetilde{\mathbf{A}}}(\widetilde{\mathbf{v}}) = \frac{\big\|\mathbf{v}\big\|^2_\varepsilon}{\big\|\mathbf{v}\big\|^2_\varepsilon + \gamma\big\|\mathbf{C}^i_E\mathbf{v}\big\|^2_\mu} \leq 1. \tag{4.15b}$$

A simple calculation shows that the inequalities (4.15) are satisfied if and only if $\rho_{\widetilde{\mathbf{A}}} \in Q$ with Q defined in (4.13a).

Next we consider only the imaginary part. Using (4.14), and (4.12) we obtain

$$0 \le \frac{\gamma}{\alpha_I}\operatorname{Im}\rho_{\widetilde{\mathbf{A}}}(\widetilde{\mathbf{v}}) = 1 + \frac{\gamma\left\|\mathbf{C}_E^e\mathbf{v}\right\|_\mu^2}{\left\|\mathbf{v}\right\|_\varepsilon^2 + \gamma\left\|\mathbf{C}_E^i\mathbf{v}\right\|_\mu^2} - \frac{\left\|\mathbf{v}\right\|_\varepsilon^2}{\left\|\mathbf{v}\right\|_\varepsilon^2 + \gamma\left\|\mathbf{C}_E^i\mathbf{v}\right\|_\mu^2} \le \Gamma_\gamma^e - \frac{1}{\Gamma_\gamma^i}. \tag{4.16}$$

The bounds (4.15a) and (4.16) are satisfied if and only if $\rho_{\widetilde{\mathbf{A}}} \in R$ with R defined in (4.13b). Hence we proved $\mathcal{F}(\widetilde{\mathbf{A}}) \subset Q \cap R$.

(b) For $\alpha_I = 0$, the matrix $\widetilde{\mathbf{A}} \in \mathbb{R}^{N\times N}$ is symmetric and thus $\rho_{\widetilde{\mathbf{A}}}(\widetilde{\mathbf{v}}) \in \mathbb{R}$ for all $\widetilde{\mathbf{v}} \in \mathbb{C}^N$. Since $\alpha = \alpha_R$ we have

$$\rho_{\widetilde{\mathbf{A}}}(\widetilde{\mathbf{v}}) = \frac{\alpha}{\gamma} + \frac{(1-\frac{\alpha}{\gamma})\left\|\mathbf{v}\right\|_\varepsilon^2 + \alpha\left\|\mathbf{C}_E^e\mathbf{v}\right\|_\mu^2}{\left\|\mathbf{v}\right\|_\varepsilon^2 + \gamma\left\|\mathbf{C}_E^i\mathbf{v}\right\|_\mu^2}. \tag{4.17}$$

If $\alpha \ge \gamma$, (4.17) can be bounded by

$$1 = \frac{\alpha}{\gamma} + \frac{(1-\frac{\alpha}{\gamma})\left\|\mathbf{v}\right\|_\varepsilon^2}{\left\|\mathbf{v}\right\|_\varepsilon^2} \le \rho_{\widetilde{\mathbf{A}}}(\widetilde{\mathbf{v}}) \le \frac{\alpha}{\gamma} + \frac{\alpha\left\|\mathbf{C}_E^e\mathbf{v}\right\|_\mu^2}{\left\|\mathbf{v}\right\|_\varepsilon^2} \le \frac{\alpha}{\gamma}\Gamma_\gamma^e,$$

Similarly, for $0 < \alpha \le \gamma$, it is straightforward to see

$$\frac{\alpha}{\gamma} \le \rho_{\widetilde{\mathbf{A}}}(\widetilde{\mathbf{v}}) \le \frac{\alpha}{\gamma} + \frac{(1-\frac{\alpha}{\gamma})\left\|\mathbf{v}\right\|_\varepsilon^2 + \alpha\left\|\mathbf{C}_E^e\mathbf{v}\right\|_\mu^2}{\left\|\mathbf{v}\right\|_\varepsilon^2} \le \Gamma_\alpha^e.$$

Furthermore, since

$$0 \le \Gamma_\gamma^e - \frac{1}{\Gamma_\gamma^i} \le \Gamma_\gamma^e, \qquad \gamma > 0,$$

all quantities defining the superset S are bounded independently of the implicitly treated mesh elements and thus, S is independent of h_f. Finally, in all cases we have $0 \notin S$. ∎

Note that the superset S derived in Theorem 4.3 is not optimal. Further, we point out that $\gamma > 0$ can be chosen freely and thus used to improve the convergence factor. For example, a natural choice would be

$$\gamma = \left|\alpha_R\right| \text{ if } \alpha_R \neq 0 \quad \text{or} \quad \gamma = \left|\alpha\right| \text{ else.} \tag{4.18}$$

In any case, one should choose $\gamma \sim \tau^2$ so that the dominating part of $\mathbf{A}$ is well approximated by the preconditioner $\mathbf{B}$.

As a special case of Theorem 4.3, we obtain an inclusion set for the field of values of $\mathbf{A}$ itself. Hence, we can state an error bound for the complex symmetric QMR method without preconditioning.

COROLLARY 4.4. *For the matrix* $\mathbf{A}$ *defined in* (3.14)*, Theorem* 4.3 *holds by substituting* $\mathbf{C}_E^e = \mathbf{C}_E$ *and* $\mathbf{C}_E^i = 0$ *in* (4.13).

Recall that by an inverse estimate [5, Lemma 1.44] there is a constant c independent of the mesh width such that $\left\|\mathbf{C}_E\right\|_{\mu\leftarrow\varepsilon} \le ch_{\min}^{-1}$. Hence, without preconditioning, the superset will scale with $h_{\min}^{-1}$. Applying Theorems 4.1 and 4.2 to the preconditioned system (4.10a) provides the following error bound:

THEOREM 4.5. *Let $\widetilde{\mathbf{x}}_m$ be the QMR approximation to the solution of (4.10). If (4.5) is satisfied, then there is a constant $\phi_0 > 1$ independent of the fine mesh such that the error of the mth pQMR iterate satisfies*

$$\left\|\widetilde{\mathbf{A}}^{-1}\widetilde{\mathbf{b}} - \widetilde{\mathbf{x}}_m\right\|_\varepsilon \le c_{\widetilde{\mathbf{A}}}(1+\sqrt{2})\big(1+(m+1)\delta\big)\min\left\{\frac{3}{\phi_0^m}, \frac{2}{\phi_0^m - 1}\right\}, \tag{4.19}$$

where

$$\begin{cases} c_{\widetilde{\mathbf{A}}} = 1, & \text{if } 0 < \gamma \le \alpha_R,\ \alpha_I = 0 \quad \text{or} \quad \alpha_I \ne 0, \\ c_{\widetilde{\mathbf{A}}} = \frac{\gamma}{\alpha_R}, & \text{if } 0 < \alpha_R \le \gamma,\ \alpha_I = 0. \end{cases} \tag{4.20}$$

Proof. Since $\widetilde{\mathbf{A}}$ is complex symmetric, we apply Theorem 4.1 for $\mathbf{K} = \widetilde{\mathbf{A}}$ with $\|\cdot\| = \|\cdot\|_\varepsilon$. By Theorem 4.3, $\mathcal{F}(\widetilde{\mathbf{A}}) \subset S$ is independent of the fine mesh and the same holds for the conformal map ϕ used in Theorem 4.2, in particular for $|\phi(0)| =: \phi_0$. Thus, the bound (4.19) follows from (4.6), (4.7), and (4.8), if we can show

$$\left\|\widetilde{\mathbf{A}}^{-1}\mathbf{w}\right\|_\varepsilon \le c_{\widetilde{\mathbf{A}}}\|\mathbf{w}\|_\varepsilon \qquad \text{for all } \mathbf{w} \in \mathbb{C}^N. \tag{4.21}$$

We choose an arbitrary $\mathbf{w} \in \mathbb{C}^N$, $\mathbf{w} \ne \mathbf{0}$ and define $\mathbf{v} = \widetilde{\mathbf{A}}^{-1}\mathbf{w}$. Then Theorem 4.3 with $c_{\widetilde{\mathbf{A}}}$ defined in (4.20) and the Cauchy-Schwarz inequality yield

$$\frac{1}{c_{\widetilde{\mathbf{A}}}} \le \operatorname{Re}\rho_{\widetilde{\mathbf{A}}}(\mathbf{v}) = \operatorname{Re}\frac{\big(\mathbf{w}, \widetilde{\mathbf{A}}^{-1}\mathbf{w}\big)_\varepsilon}{\left\|\widetilde{\mathbf{A}}^{-1}\mathbf{w}\right\|_\varepsilon^2} \le \frac{\|\mathbf{w}\|_\varepsilon\left\|\widetilde{\mathbf{A}}^{-1}\mathbf{w}\right\|_\varepsilon}{\left\|\widetilde{\mathbf{A}}^{-1}\mathbf{w}\right\|_\varepsilon^2} = \frac{\|\mathbf{w}\|_\varepsilon}{\left\|\widetilde{\mathbf{A}}^{-1}\mathbf{w}\right\|_\varepsilon}. \tag{4.22}$$

This proves (4.21). ∎

As an immediate consequence of Theorem 4.5 we see that the error of the pQMR method is bounded independently of the fine mesh, since S only depends on the coarse mesh. In particular, the number of iterations is uniformly bounded with respect to further refinement of the fine part of the mesh.

5. Numerical experiments. For our numerical experiments, we consider the transverse magnetic (TM) polarization of linear Maxwell's equations (2.1) in a homogeneous medium with $\mu = \epsilon = 1$ in a square $\Omega = (-1,1)^2 \subset \mathbb{R}^2$, i.e.,

$$\begin{aligned} \partial_t H_x(t) &= -\partial_y E_z(t), \\ \partial_t H_y(t) &= \ \ \partial_x E_z(t), \\ \partial_t E_z(t) &= -\partial_y H_x(t) + \partial_x H_y(t) - J_z(t), \\ H_x(0) = H_x^0, &\quad H_y(0) = H_y^0, \quad E_z(0) = E_z^0. \end{aligned} \tag{5.1}$$

As an example of locally refined meshes, we consider a series of unstructured meshes as depicted in Figure 5.1, cf. [25] for more details.

We start with the initial mesh in Figure 5.1a, which is divided into two parts: an inner fine mesh $\mathcal{T}_{h,f}$ in the green square $[-0.05, 0.05]^2$ and an outer coarse mesh $\mathcal{T}_{h,c}$ in $[-1,1]^2 \backslash [-0.05, 0.05]^2$. We call this mesh $\mathcal{T}_{h,f}^{(1)}$, where the superscript denotes the level of refinement of the fine mesh. We keep the coarse part the same but refine the innermost part of the fine meshes recursively to produce three new meshes $\mathcal{T}_{h,f}^{(2)}, \mathcal{T}_{h,f}^{(3)}, \mathcal{T}_{h,f}^{(4)}$. The fine parts of all four meshes are shown in Figure 5.1b. Based on this decomposition, the split curl matrices $\mathbf{C}_E^i, \mathbf{C}_H^i$ act on the fine mesh elements

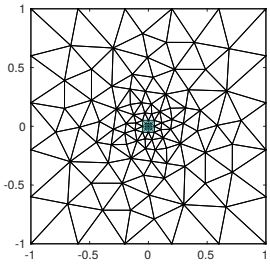

(a) Mesh $\mathcal{T}_{h,f}^{(1)}$ with fine mesh of refinement level 1.

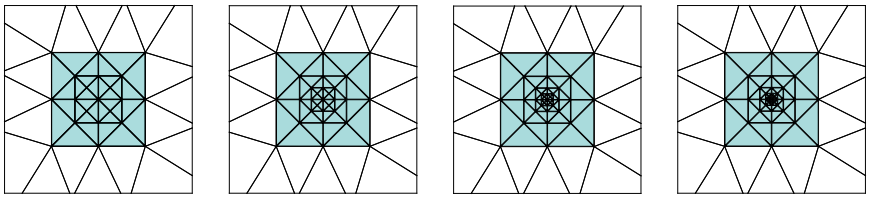

(b) Refinement of the elements in $\mathcal{T}_{h,f}$: from left to right $\mathcal{T}_{h,f}^{(1)}, \ldots, \mathcal{T}_{h,f}^{(4)}$.

Fig. 5.1: Illustration of mesh refinements.

and their direct neighbors, while $\mathbf{C}_E^e, \mathbf{C}_H^e$ act on the remaining coarse mesh elements. The codes for these experiments are available at [27].

Furthermore, for all these experiments we fix

$$\alpha = \Big(\frac{1}{24} + i\frac{\sqrt{3}}{24}\Big)\tau^2, \qquad \gamma = \alpha_R = \frac{\tau^2}{24}, \tag{5.2}$$

for $\mathbf{A}$ in (3.14) and the preconditioner $\mathbf{B}$ in (4.9) respectively. This choice of α corresponds to (3.12), where λ_i is one of the two complex conjugate eigenvalues of the RK matrix $\boldsymbol{\mathcal{O}}$ of the fourth-order implicit Gauß-Legendre RK method.

In the first experiment, we consider the locally refined mesh in Figure 5.1a, and construct $\widetilde{\mathbf{A}}$ with α, γ defined in (5.2) for different choices of τ. We then compute the boundary of $\mathcal{F}(\widetilde{\mathbf{A}})$ using the matlab function `wber.m` from [30], and the superset S derived in Theorem 4.3. In Figure 5.2, we observe that $\mathcal{F}(\widetilde{\mathbf{A}}) \subseteq S$ for all considered values of $\tau = 0.1, 0.01, 0.001$, and hence numerically verify Theorem 4.3. Moreover, the superset S is close to being optimal for $\tau = 0.1$ and $\tau = 0.001$, but not for $\tau = 0.01$. Clearly, for $\tau \to 0$, $\mathcal{F}(\widetilde{\mathbf{A}}) \to \{1\}$.

Next, we numerically calculate an optimized value γ_{opt} of γ used in the definition of the preconditioner $\mathbf{B}$ in (4.9). For the mesh in Figure 5.1a, we choose α in (5.2) with $\tau = 0.05$, and compute ϕ_0 defined in Theorem 4.5 using the Schwarz–Christoffel toolbox [7]. In Figure 5.3, we plot $1/\phi_0$ for different values of γ, and observe that $1/\phi_0$ for $\gamma_{\text{opt}} \approx 3.7\text{e}{-5}$ and $\gamma = \alpha_R \approx 1\text{e}{-4}$ are close to each other. This suggests that $\gamma \approx \alpha_R$ for $\alpha_R > 0$ could be a good guess for γ_{opt}.

We then examine the number of iterations required by QMR and pQMR to solve the linear system (3.14) up to a tolerance of 10^{-3} in $\|\cdot\|_\varepsilon$. The coefficient matrix $\mathbf{A}$ and the preconditioner $\mathbf{B}$ are constructed with α, γ in (5.2) for $\tau = 0.05$ on the meshes $\mathcal{T}_{h,f}^{(1)}, \ldots, \mathcal{T}_{h,f}^{(4)}$ depicted in Figure 5.1. For this experiment, we fix random vectors $\mathbf{x}_0$

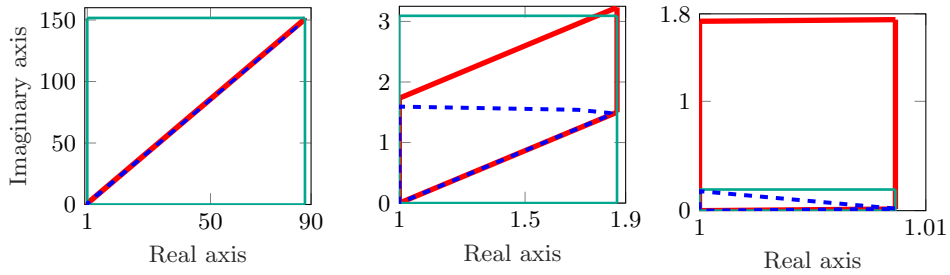

Fig. 5.2: Boundary of a numerical approximation of $\mathcal{F}(\widetilde{\mathbf{A}})$ in blue, quadrilaterals Q and R in red and green, respectively, for $\tau = 0.1, 0.01, 0.001$ (from left to right).

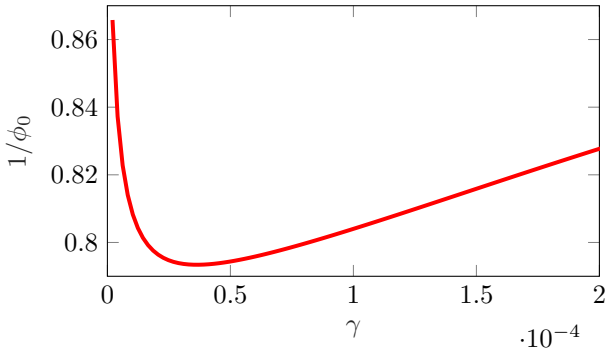

Fig. 5.3: Dependence of ϕ_0 on γ for α in (5.2) with $\tau = 0.05$.

and $\mathbf{b}$. In Figure 5.4, we plot their relative errors against number of iterations m. We observe that for all meshes, pQMR requires same number of iterations to reach the tolerance. In contrast, the number of iterations without preconditioning grows as the fine mesh is refined, as expected.

It remains to verify the error bounds presented in Theorem 4.5. To do so, we consider the mesh in Figure 5.1a and solve the preconditioned linear system (4.10a) for a fixed time step $\tau = 0.01$, α, γ given in (5.2), and fixed random vectors $\mathbf{b}, \mathbf{x}_0$. Figure 5.5 numerically verifies the error bounds produced by Theorem 4.5 for differently calculated values of ϕ_0 for the pQMR method.

6. Conclusion. In this paper, we proposed and analyzed computationally efficient implicit higher-order time integration methods for solving linear Maxwell's equations on locally refined spatial grids which consist of a small number of fine and a large number of coarse mesh elements. This is achieved by constructing a preconditioned Krylov subspace method for solving the linear systems arising in each time step of the implicit scheme. Our main result shows that the number of Krylov steps to achieve the desired accuracy can be bounded independently of the fine mesh.

Although we focused on linear Maxwell's equations, our ideas carry over to nonlinear problems, where linear systems of the same type appear in each iteration of a (simplified) Newton method. Moreover, instead of Gauß collocation methods other implicit time integration schemes might be employed and the preconditioner can also be combined with rational Krylov subspace methods.

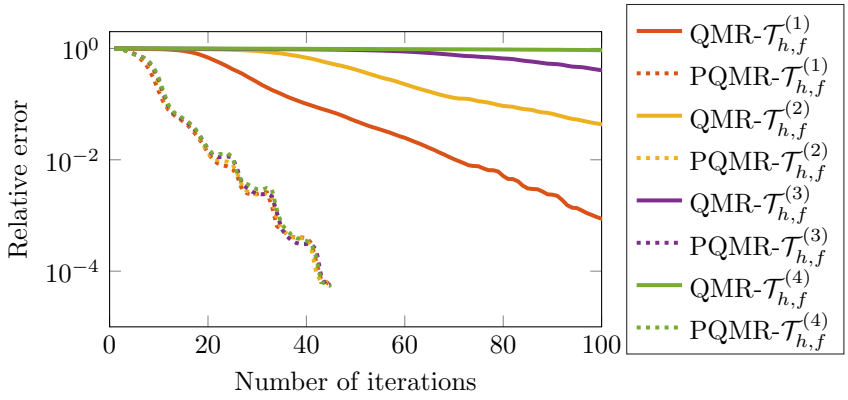

Fig. 5.4: Relative error of QMR (solid lines) and pQMR (dashed lines) for different levels of fine mesh refinement.

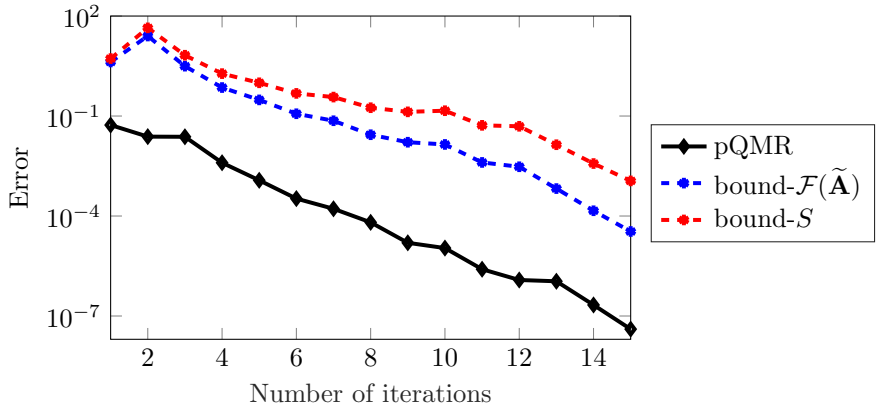

Fig. 5.5: Error produced by pQMR in black and its bound when ϕ_0 is calculated using a numerical approximation to $\mathcal{F}(\widetilde{\mathbf{A}})$ in blue while that calculated using the polygon S in red.

REFERENCES

[1] J. Chabassier and S. Imperiale, *Fourth-order energy-preserving locally implicit time discretization for linear wave equations*, International Journal for Numerical Methods in Engineering, 106 (2016), pp. 593–622, https://onlinelibrary.wiley.com/doi/abs/10.1002/nme.5130.

[2] M. Crouzeix and C. Palencia, *The numerical range is a* $(1+\sqrt{2})$*-spectral set*, SIAM J. Matrix Anal. Appl., 38 (2017), pp. 649–655, https://doi.org/10.1137/17M1116672, https://doi.org/10.1137/17M1116672.

[3] S. Descombes, S. Lanteri, and L. Moya, *Locally Implicit Time Integration Strategies in a Discontinuous Galerkin Method for Maxwell's Equations*, Journal of Scientific Computing, 56 (2013), pp. 190–218, https://doi.org/10.1007/s10915-012-9669-5.

[4] S. Descombes, S. Lanteri, and L. Moya, *Temporal convergence analysis of a locally implicit discontinuous Galerkin time domain method for electromagnetic wave propagation in dispersive media*, Journal of Computational and Applied Mathematics, 316 (2017), pp. 122–132, https://www.sciencedirect.com/science/article/pii/S0377042716304587.

[5] D. A. Di Pietro and A. Ern, *Mathematical Aspects of Discontinuous Galerkin Methods*, vol. 69 of Mathématiques et Applications, Springer-Verlag Berlin Heidelberg, 2012, https://www.springer.com/gp/book/9783642229794.

[6] J. Diaz and M. J. Grote, *Energy Conserving Explicit Local Time Stepping for Second-Order Wave Equations*, SIAM Journal on Scientific Computing, 31 (2009), pp. 1985–2014, https://doi.org/10.1137/070709414.

[7] T. A. Driscoll, *Algorithm 756: a MATLAB toolbox for Schwarz-Christoffel mapping*, ACM Trans. Math. Softw., 22 (1996), pp. 168–186, https://dl.acm.org/doi/10.1145/229473.229475.

[8] T. A. Driscoll, *Algorithm 843: improvements to the Schwarz-Christoffel toolbox for MATLAB*, ACM Trans. Math. Software, 31 (2005), pp. 239–251, https://doi.org/10.1145/1067967.1067971, https://doi.org/10.1145/1067967.1067971.

[9] M. Eiermann, *On semi-iterative methods generated by Faber polynomials*, Numer. Math, 56 (1989), pp. 139–156, https://doi.org/10.1007/BF01409782.

[10] R. W. Freund, *Conjugate gradient-type methods for linear systems with complex symmetric coefficient matrices*, SIAM J. Sci. Statist. Comput., 13 (1992), pp. 425–448, https://doi.org/10.1137/0913023, https://doi.org/10.1137/0913023.

[11] R. W. Freund, G. H. Golub, and N. M. Nachtigal, *Iterative solution of linear systems*, in Acta numerica, 1992, Acta Numer., Cambridge Univ. Press, Cambridge, 1992, pp. 57–100, https://doi.org/10.1017/s0962492900002245, https://doi.org/10.1017/s0962492900002245.

[12] R. W. Freund, M. H. Gutknecht, and N. M. Nachtigal, *An Implementation of the Look-Ahead Lanczos Algorithm for Non-Hermitian Matrices*, SIAM Journal on Scientific Computing, 14 (1993), pp. 137–158, https://doi.org/10.1137/0914009.

[13] R. W. Freund and N. M. Nachtigal, *QMR: a quasi-minimal residual method for non-Hermitian linear systems*, Numerische Mathematik, 60 (1991), pp. 315–339, https://link.springer.com/article/10.1007/BF01385726.

[14] R. W. Freund and N. M. Nachtigal, *An implementation of the QMR method based on coupled two-term recurrences*, SIAM J. Sci. Comput., 15 (1994), pp. 313–337, https://doi.org/10.1137/0915022, https://doi.org/10.1137/0915022. Iterative methods in numerical linear algebra (Copper Mountain Resort, CO, 1992).

[15] M. J. Grote, M. Mehlin, and T. Mitkova, *Runge–Kutta-Based Explicit Local Time-Stepping Methods for Wave Propagation*, SIAM Journal on Scientific Computing, 37 (2015), pp. A747–A775, https://doi.org/10.1137/140958293.

[16] M. J. Grote and T. Mitkova, *Explicit local time-stepping methods for Maxwell's equations*, Journal of Computational and Applied Mathematics, 234 (2010), pp. 3283–3302, https://www.sciencedirect.com/science/article/pii/S0377042710002360.

[17] M. H. Gutknecht, *Lanczos-type solvers for nonsymmetric linear systems of equations*, in Acta numerica, 1997, vol. 6 of Acta Numer., Cambridge Univ. Press, Cambridge, 1997, pp. 271–397, https://doi.org/10.1017/S0962492900002737, https://doi.org/10.1017/S0962492900002737.

[18] E. Hairer, C. Lubich, and G. Wanner, *Geometric Numerical Integration*, vol. 31 of Springer Series in Computational Mathematics, Springer-Verlag Berlin Heidelberg, 2006, https://link.springer.com/book/10.1007/3-540-30666-8.

[19] E. Hairer and G. Wanner, *Solving Ordinary Differential Equations II*, vol. 14 of Springer Series in Computational Mathematics, Springer-Verlag Berlin Heidelberg, 1996, https://www.springer.com/de/book/9783540604525.

[20] M. Hochbruck and J. Köhler, *Error Analysis of Discontinuous Galerkin Discretizations of a Class of Linear Wave-type Problems*, in Mathematics of Wave Phenomena, W. Dörfler, M. Hochbruck, D. Hundertmark, W. Reichel, A. Rieder, R. Schnaubelt, and B. Schörkhuber, eds., Cham, 2020, Springer International Publishing, pp. 197–218, https://link.springer.com/chapter/10.1007%2F978-3-030-47174-3_12.

[21] M. Hochbruck and J. Köhler, *Wave Phenomena: Mathematical Analysis and Numerical Approximation*, vol. 49 of Oberwolfach Seminars, Birkhäuser Cham, 2022, ch. Time integration for dG discretizations of Friedrichs' systems. to appear.

[22] M. Hochbruck and C. Lubich, *On Krylov subspace approximations to the matrix exponential operator*, SIAM J. Numer. Anal., 34 (1997), pp. 1911–1925, http://dx.doi.org/10.1137/S0036142995280572.

[23] M. Hochbruck and C. Lubich, *Error Analysis of Krylov Methods In a Nutshell*, SIAM Journal on Scientific Computing, 19 (1998), pp. 695–701, https://epubs.siam.org/doi/10.1137/S1064827595290450.

[24] M. Hochbruck and T. Pazur, *Implicit Runge–Kutta Methods and Discontinuous Galerkin Discretizations for Linear Maxwell's Equations*, SIAM Journal on Numerical Analysis, 53

(2015), pp. 485–507, https://doi.org/10.1137/130944114.
[25] M. Hochbruck and A. Sturm, *Error Analysis of a Second-Order Locally Implicit Method for Linear Maxwell's Equations*, SIAM J. Numer. Anal., 54 (2016), pp. 3167–3191, https://doi.org/10.1137/15M1038037.
[26] M. Hochbruck and A. Sturm, *Upwind discontinuous Galerkin space discretization and locally implicit time integration for linear Maxwell's equations*, Math. Comp., 88 (2019), pp. 1121–1153, https://doi.org/10.1090/mcom/3365.
[27] P. M. Kumbhar, *Codes for numerical experiments*, 2022, https://github.com/Pratikk17/preconditioned_implicit/releases/tag/v1.0.
[28] S. Piperno, *Symplectic local time-stepping in non-dissipative DGTD methods applied to wave propagation problems*, ESAIM: M2AN, 40 (2006), pp. 815–841, https://doi.org/10.1051/m2an:2006035.
[29] Y. Saad, *Iterative Methods for Sparse Linear Systems*, Graduate Studies in Mathematics, Society for Industrial and Applied Mathematics, second ed., 2003, https://epubs.siam.org/doi/book/10.1137/1.9780898718003?mobileUi=0.
[30] F. Uhlig, *MATLAB m -file wber3.m.*, 2012, http://webhome.auburn.edu/~uhligfd/m_files/.
[31] J. G. Verwer, *Component splitting for semi-discrete Maxwell equations*, BIT Numerical Mathematics, 51 (2011), pp. 427–445, https://doi.org/10.1007/s10543-010-0296-y.
[32] K. Yee, *Numerical solution of initial boundary value problems involving Maxwell's equations in isotropic media*, IEEE Transactions on Antennas and Propagation, 14 (1966), pp. 302–307, https://ieeexplore.ieee.org/document/1138693.